Rapid Communications

Theoretical investigation of superconductivity in trilayer square-planar nickelates

Emilian M. Nica,[1,*] Jyoti Krishna,[1] Rong Yu,[2] Qimiao Si,[3,4] Antia S. Botana,[1,†] and Onur Erten[1]

[1]*Department of Physics, Arizona State University Tempe, Arizona 85287-1504, USA*

[2]*Department of Physics, Renmin University of China, 59 Zhongguancun St, Beijing, 100872 China*

[3]*Department of Physics and Astronomy, Rice University, 6100 Main St, Houston, Texas 77005, USA*

[4]*Rice Center for Quantum Materials, Rice University, 6100 Main St, Houston, Texas 77005, USA*

(Received 24 March 2020; accepted 6 July 2020; published 27 July 2020)

The discovery of superconductivity in Sr-doped $NdNiO_2$ is a crucial breakthrough in the long pursuit for nickel oxide materials with electronic and magnetic properties similar to those of the cuprates. $NdNiO_2$ is the infinite-layer member of a family of square-planar nickelates with general chemical formula $R_{n+1}Ni_nO_{2n+2}$ (R = La, Pr, Nd, $n = 2, 3, \ldots \infty$). In this Rapid Communication, we investigate superconductivity in the trilayer member of this series ($R_4Ni_3O_8$) using a combination of first-principles and $t-J$ model calculations. $R_4Ni_3O_8$ compounds resemble cuprates more than $RNiO_2$ materials in that only Ni-$d_{x^2-y^2}$ bands cross the Fermi level, they exhibit a largely reduced charge transfer energy, and as a consequence superexchange interactions are significantly enhanced. We find that the superconducting instability in doped $R_4Ni_3O_8$ compounds is considerably stronger with a maximum gap about four times larger than that in $Sr_{0.2}Nd_{0.8}NiO_2$.

DOI: 10.1103/PhysRevB.102.020504

Understanding the mechanism behind high-temperature superconductivity (HTS) in the cuprate family remains one of the main challenges in condensed matter physics [1]. One way of addressing this open question has been to search for cuprate analogs that display the properties deemed relevant to HTS: a layered structure similar to that of the CuO_2 planes, d^9 spin-1/2 ions, strong antiferromagnetic (AFM) correlations, isolated $d_{x^2-y^2}$ bands near the Fermi energy, and strong $p-d$ hybridization. Therefore, Ni-based compounds have been promising candidates since Ni^{1+} and Cu^{2+} are isoelectronic d^9 ions [2]. A Ni^{1+} oxidation state is indeed realized in square-planar infinite-layer systems $RNiO_2$ (R = La, Nd). After more than three decades of effort [3–7], superconductivity in $NdNiO_2$ (112) films was recently observed upon Sr doping with $T_c \sim 15$ K [8].

First-principles calculations reveal similarities as well as differences between the parent infinite-layer 112 compound $NdNiO_2$ and members of the cuprate family [9–18]. While a single Ni-$d_{x^2-y^2}$ band indeed crosses the Fermi level as in the cuprates, R-d electron pockets are also present. These likely prevent the parent phase from becoming a simple Mott insulator and suggest that Kondo interactions may play a relevant role [12]. Nonetheless, Sr-doped 112 compounds have a Fermi surface which is similar to that of the cuprates and several authors have proposed an analogous $d_{x^2-y^2}$ pairing order parameter [14,19]. Reference [20] argues that interfacial effects may suppress R-d pockets and give rise to a picture that includes only Ni-$d_{x^2-y^2}$ features supplemented by interfacial Ni-d_{z^2} flat bands.

Importantly, 112 nickelates are the infinite-layer members of a larger series represented by the general formula $R_{n+1}Ni_nO_{2n+2}$ (R = La, Pr, Nd, $n = 2; 3; \ldots \infty$) with each member containing n-NiO_2 layers [21,22]. The materials in this series are obtained via oxygen reduction from perovskite-like parent phases [21,22] as shown in Fig. 1. The fact that 112 nickelates belong to this larger series suggests the existence of a cupratelike family of nickelate HTS.

Among the other members of this nickelate family, the trilayer materials $R_4Ni_3O_8$ (438) and especially $Pr_4Ni_3O_8$ have already been defined as close analogs of the cuprates, therefore, promising candidates for HTS [23,24]. The structure of the $n = 3$ and $n = \infty$ layered materials and their corresponding parent phases are shown in Fig. 1. In 112 compounds, adjacent NiO_2 planes are separated by a single layer of rare-earth ions. 438 compounds exhibit trilayer blocks with an analogous structure. However, each of these blocks is separated along the c axis by a fluorite slab formed by rare-earth and oxygen ions. For the 438 materials, an average Ni valence of 1.33+ ($d^{8.67}$) is obtained [23]. In terms of d filling, 438 compounds can be mapped onto the overdoped regime of the cuprate phase diagram [25] suggesting that HTS could be accessible via electron doping using, i.e., Ce^{4+} [24]. So far, experimental reports attempting doping have used isoelectronic substitution on the rare-earth site or changes on the Ni planes [26–28]. To determine if electron doping can give rise to HTS in the trilayer 438 materials, we study the electronic structure and superconductivity in a $t-J$ model for the 438 trilayer nickelates. We also analyze a related $t-J$ model for the 112 compounds in order to provide a reference within the Ni-based family. We find robust $d_{x^2-y^2}$-wave superconductivity in the 438 materials upon electron doping, with a maximum $T_c \sim 90$ K, much larger than the 112 material as a consequence of an enhanced superexchange interaction.

We performed density functional theory (DFT)-based calculations for 438 and 112 nickelates using the all-electron,

*Corresponding author: enica@asu.edu

†Corresponding author: antia.botana@asu.edu

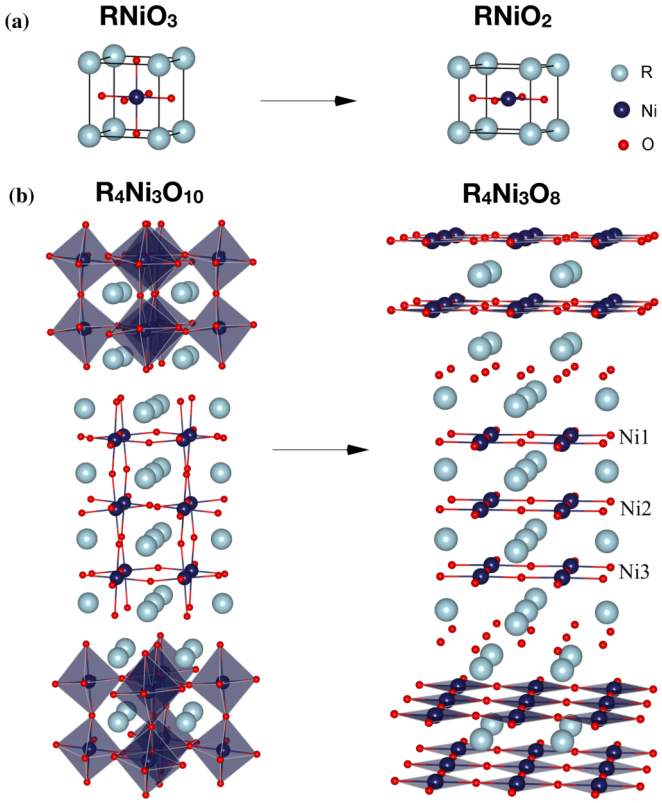

FIG. 1. Crystal structure of 112 and 438 square-planar nickelates (right panels). These compounds are obtained via oxygen reduction from the corresponding 113 and 4310 perovskitelike parent compounds (left panels). Oxygen, rare-earth (R), and nickel atoms are depicted in red, light blue, and dark blue, respectively.

full potential code WIEN2K [29] based on the augmented plane wave plus local orbitals (APW + lo) basis set. The Perdew-Burke-Ernzerhof version of the generalized gradient approximation (GGA) [30] was used for the paramagnetic calculations. More details on the simulations are provided in Ref. [31]. To avoid issues connected with Nd- and Pr-4f states, we perform calculations for $LaNiO_2$ and $La_4Ni_3O_8$, with lattice parameters adopted from $NdNiO_2$ and $Pr_4Ni_3O_8$, respectively. The extraction of tight binding parameters for $t-J$ models is based on the Wannier functions formalism [32,33]. Hopping coefficients and on-site energies obtained from the Wannier fits for the 438 compounds are shown in Table I of Ref. [31].

Figure 2 shows the paramagnetic band structures and orbital-projected density of states (DOS) of La112 (d^9) and La438 ($d^{8.67}$). In the 112 case shown in Fig. 1(a) the Ni-$d_{x^2-y^2}$ band crosses the Fermi level. However, as determined in previous work [9–13,16], additional Nd-5d bands also contribute to the Fermi surface, giving rise to two electron pockets that self-dope the $d_{x^2-y^2}$ band [see Fig. 2(c)]. The pockets at Γ and A have predominant Nd-d_{z^2} and Nd-d_{xy} character, respectively. The large separation in energy between O-p and Ni-d bands is apparent from the DOS, as shown in the right panel. The corresponding charge transfer energy $\Delta = E_d - E_p$ is derived from the values of the onsite energies for the Wannier functions as $\Delta_{112} \sim 4.4$ eV.

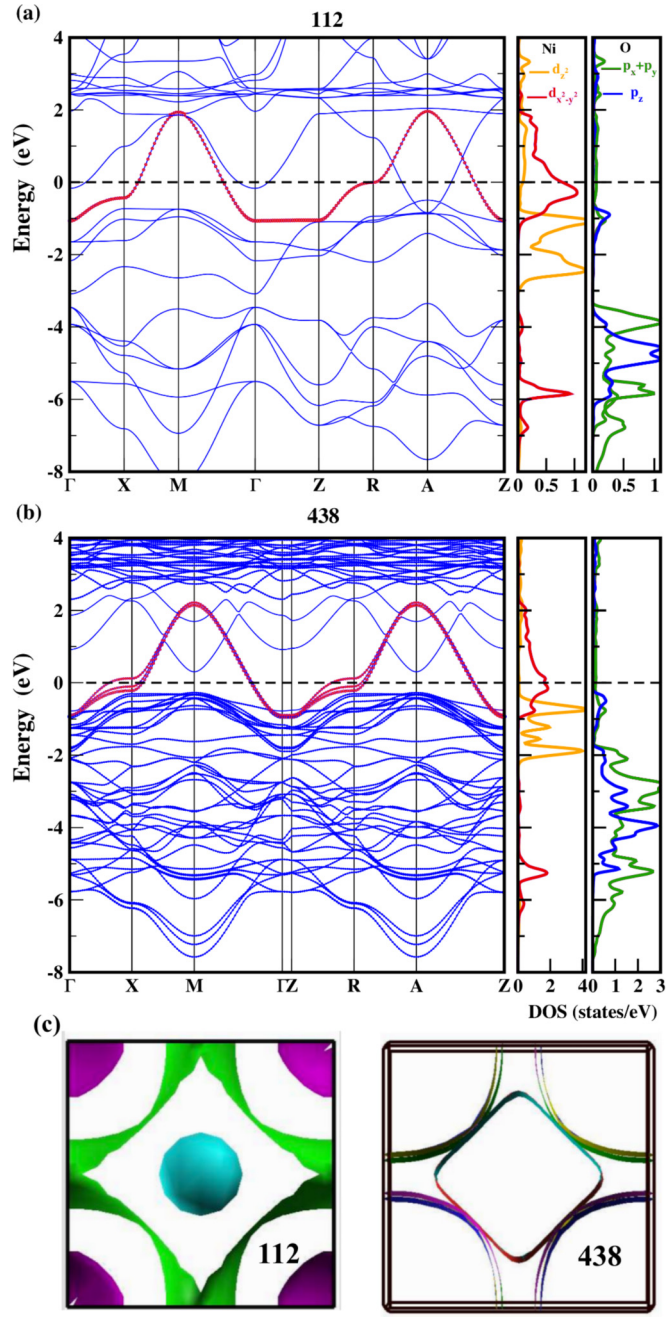

FIG. 2. Band structure and orbital projected DOS for (a) 112 and (b) 438 compounds. Bands with Ni-$d_{x^2-y^2}$ character crossing the Fermi level are shown in red. The right panels show the Ni $d_{x^2-y^2}$ and d_{z^2} and O p_x, p_y, and p_z orbital projected DOS. Panel (c) shows the corresponding Fermi surfaces.

The band structure for the 438 compounds shown in Fig. 2(b) differs significantly from that of the 112's. Only a single Ni $d_{x^2-y^2}$ band per Ni crosses the Fermi level in analogy to the cuprates but in sharp contrast to the 112 compounds. The R-d bands are displaced to roughly 0.5 eV above the Fermi level. A splitting between the three Ni-$d_{x^2-y^2}$ bands is observed at X as a consequence of interlayer hopping similar to that in multilayer cuprates [34]. The corresponding Fermi surface [shown in Fig. 2(c)] resembles that of heavily

hole-doped cuprates bearing one electron pocket (coming from the inner Ni) and two hole pockets (from the outer ones).

More importantly, the charge transfer energy is largely reduced in the 438 compounds, $\Delta_{438} \sim 3.4$ eV, 1 eV smaller than that of the 112 material. The difference in charge transfer energies between the 112 and 438 cases is consistent with x-ray absorption experiments [23]. While a pre-peak is observed in the 438 materials at the O-K edge, indicative of oxygen holes, no such pre-peak is observed in the 112 materials [12]. The in-plane $p-d$ hopping coefficients in 112 [10] and 438 materials (see Ref. [31]) are almost identical.

The difference in charge transfer energies between the 438 and 112 materials significantly impacts the corresponding nearest-neighbor (NN) superexchange coupling J. For 112 materials, the J determined by experiments [35] is ~25 meV, a quarter of the value characteristic of the cuprates. Here, we estimate J in the 438 case theoretically using an expression [36] which includes both the Mott and charge transfer limits:

$$J_{dd} = \frac{2t_{pd}^4}{\Delta^2 U_{dd}} + \frac{4t_{pd}^4}{\Delta^2(2\Delta + U_{pp})}. \tag{1}$$

Our estimates of Δ_{438} and t_{pd} together with values of U_{pp} and U_{dd} characteristic of the cuprates [37], lead to $J \approx 80$ meV. *Ab initio* calculations show that Ce-doped $Pr_4Ni_3O_8$ has the same electronic structure as the antiferromagnetic insulating phase of parent cuprates at half filling. For this system ($CePr_3Ni_3O_8$, d^9) a similar value of J is derived by fitting the energies of different magnetic configurations to a Heisenberg model [24].

We now consider effective $t-J$ models for these two materials. While our focus is on the 438 case, we also provide results for the 112 case, as a reference within the Ni-based family. For the 438 case, we consider an effective three Ni-d orbital $t-J$ model:

$$\begin{aligned} H &= P_s(H_t + H_J)P_s \\ H_t &= -\sum_{\substack{ij \\ \alpha\beta,\sigma}} \left(t_{ij}^{\alpha\beta} c_{i\alpha\sigma}^\dagger c_{j\beta\sigma} + \text{H.c.}\right) - \mu \sum_{i,\alpha,\sigma} c_{i\alpha\sigma}^\dagger c_{i\alpha\sigma} \\ H_J &= \sum_{\langle ij\rangle,\alpha} J_{ij}^{\alpha\alpha}\left(\boldsymbol{S}_{i\alpha}\cdot\boldsymbol{S}_{j\alpha} - \frac{n_{i\alpha}n_{j\alpha}}{4}\right) \\ &\quad + \sum_{\alpha<\beta,i} J_{ii}^{\alpha\beta}\left(\boldsymbol{S}_{i\alpha}\cdot\boldsymbol{S}_{i\beta} - \frac{n_{i\alpha}n_{i\beta}}{4}\right). \end{aligned} \tag{2}$$

The indices i, j cover a two-dimensional square lattice, as the weak dispersion along the c axis is neglected. The indices $\alpha, \beta \in \{1, 2, 3\}$ label the Ni $d_{x^2-y^2}$ orbitals in each of the three NiO_2 layers. The projection operator P_s enforces the exclusion of doubly-occupied states in each Ni sector for hole doping. A similar model is used for electron doping, as discussed in Ref. [31].

To capture the DFT bands, NN, next-NN (NNN), and third-NN in-plane hopping terms are included $t_{xx}^{\alpha\alpha} = 390$ meV, $t_{xy}^{\alpha\alpha} = -100$ meV, $t_{xxy}^{\alpha\alpha} = 41$ meV, which are identical for all Ni sectors. The splitting between the three Ni bands is due to an interlayer hybridization $-2t^{\alpha\beta}(\cos(k_x a) - \cos(k_y a))^2$, where $t^{\alpha\beta} = 16$ meV is used as obtained from DFT calculations for $(\alpha, \beta) \in \{(1, 2), (2, 3)\}$. These interlayer terms are typical in multilayered cuprates [31]. As NN intralayer exchange we use the $J_{ij}^{\alpha\alpha} = J_\parallel = 80$ meV value derived previously. Local, interlayer exchanges are also included $J_{ii}^{\alpha\beta} = J_z = 17$ meV for $(\alpha, \beta) \in \{(1, 2), (2, 3)\}$, identical for each pair of interlayer Ni orbitals.

A slave-boson representation for each Ni orbital is introduced [38] and solutions at $T = 0$ which preserve time reversal as well as all of the symmetries of the lattice are considered. In addition to the usual Gutzwiller condition, the filling in each Ni sector is also fixed, as determined from the noninteracting bands. This condition is the main approximation of our model, as described in Ref. [31]. Consequently, at $T = 0$, the boson in each sector $\langle b_{i\alpha}^\dagger\rangle$, $\langle b_{i\alpha}\rangle$ can be replaced by $b_\alpha = \sqrt{\delta_\alpha}$, where δ_α is the hole doping of the Ni $d_{x^2-y^2}$ in layer α. Within a Hartree-Fock self-consistent approach, we also decouple the exchange interactions in NN intralayer and local interlayer particle-particle (p-p) and particle-hole (p-h) channels

$$B_{\boldsymbol{e}}^{(\alpha\alpha)} = \frac{2}{N_s}\sum_{\boldsymbol{k}} \cos(\boldsymbol{k}\cdot\boldsymbol{e})\,\langle f_{\boldsymbol{k}\alpha\downarrow} f_{-\boldsymbol{k}\alpha\uparrow}\rangle \tag{3}$$

$$B^{(\alpha\beta)} = \frac{1}{N_s}\sum_{\boldsymbol{k}} \langle f_{\boldsymbol{k}\alpha\downarrow} f_{-\boldsymbol{k}\beta\uparrow} + f_{\boldsymbol{k}\beta\downarrow} f_{-\boldsymbol{k}\alpha\uparrow}\rangle \tag{4}$$

$$\chi_{\boldsymbol{e}}^{(\alpha\alpha)} = \frac{1}{N_s}\sum_{\boldsymbol{k}}\sum_{\sigma} e^{i\boldsymbol{k}\cdot\boldsymbol{e}}\,\langle f_{\boldsymbol{k}\alpha\sigma}^\dagger f_{\boldsymbol{k}\alpha\sigma}\rangle \tag{5}$$

$$\chi^{(\alpha\beta)} = \frac{1}{N_s}\sum_{\boldsymbol{k}}\sum_{\sigma} \langle f_{\boldsymbol{k}\alpha\sigma}^\dagger f_{\boldsymbol{k}\beta\sigma}\rangle\,, \tag{6}$$

where N_s denotes the number of sites of the 2D lattice, $\boldsymbol{e} \in \{\hat{\boldsymbol{x}}, \hat{\boldsymbol{y}}\}$ is the NN intralayer separation, and $f_{\boldsymbol{k}\alpha\sigma}$ is the electron operator in the α sector within the slave-boson representation.

To study the effects of doping in the 112 material, we consider an effective $t-J$ model involving the Ni and two rare-earth Nd d bands which cross the Fermi energy [14]. Exchange couplings and projection of doubly-occupied states are in effect only for the Ni $d_{x^2-y^2}$ orbital. As in the 438 case, we fix the filling of the Ni orbital from the noninteracting bands and decouple into p-p and p-h channels within a slave-boson representation. Our procedure incorporates the effects of interactions via band renormalization [38] as in similar approaches for the cuprates, while retaining realistic values of the exchange coupling constants [31].

In Fig. 3(a), we present the pairing amplitude or gap order parameters in the $d_{x^2-y^2}$ irreducible representation at $T = 0$ for the three Ni orbitals in the 438 case as functions of their respective dopings δ_α with respect to the half-filled system $CeR_3Ni_3O_8$ (d^9) . The position of the parent $R_4Ni_3O_8$ phase ($d^{8.67}$) is also shown. The gap order parameters are determined from

$$\Delta_{d_{x^2-y^2}\alpha} = \frac{3J_\parallel}{4}\left(B_{\hat{\boldsymbol{x}}}^{\alpha\alpha} - B_{\hat{\boldsymbol{y}}}^{\alpha\alpha}\right). \tag{7}$$

The intralayer pairings in the $s_{x^2+y^2}$ channels, as well as all of the interlayer pairing channels, are strongly suppressed in the doping regimes shown here. Similarly, all of the interlayer $T = 0$ p-h mean-field parameters are suppressed relative to the intralayer values (see Ref. [31]). The amplitudes for $d_{x^2-y^2}$ pairing in the three Ni sectors shown in Fig. 3(a) follow a very similar evolution with doping. The slight anisotropy in

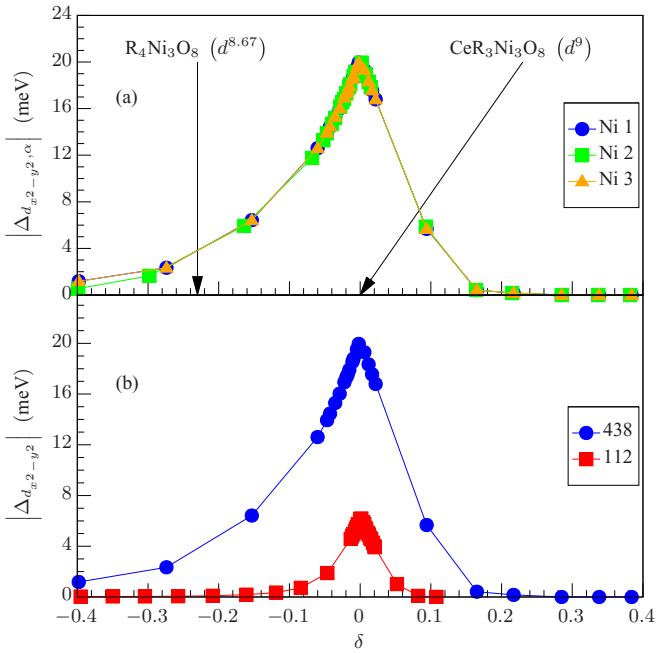

FIG. 3. (a) Pairing amplitudes at $T = 0$ for the 438 compounds in the $d_{x^2-y^2}$ channel as a function of doping for each of the Ni orbitals as determined from Eq. (7). The arrows show the compound at half filling $CeR_3Ni_3O_8$ (d^9) and the parent phase $R_4Ni_3O_8$ $(d^{8.67})$. Ni1 and Ni3 occupy the outer layers while Ni2 occupies the inner layer as shown in Fig. 1. The amplitudes in each Ni sector are similar. The offsets which are visible at lower hole dopings are due to interlayer coupling. (b) Pairing amplitude at $T = 0$ for the 438 family in the $d_{x^2-y^2}$ channel in the Ni sector (blue circles) and pairing amplitude for the 112 family in the $d_{x^2-y^2}$ channel for Ni (red squares). Both are plotted as functions of their respective dopings. The leading pairing channel for the 438 case is roughly four times larger than that for the 112 case.

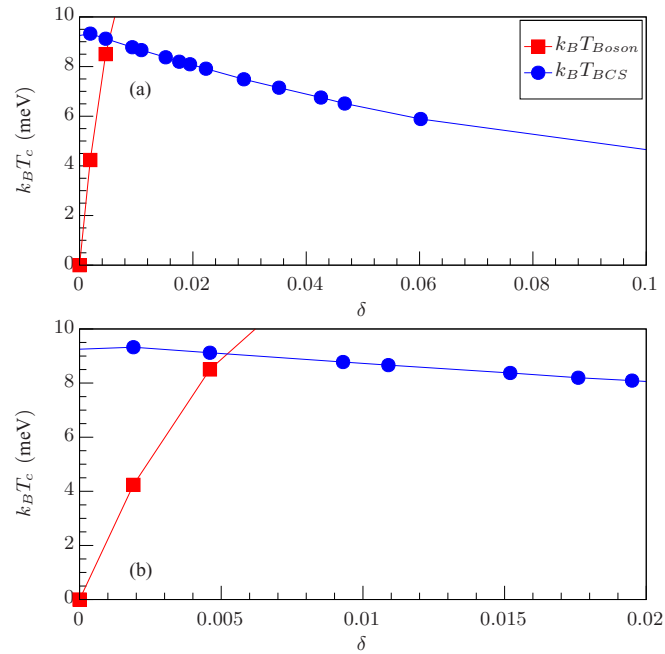

FIG. 4. (a) Estimate of the superconducting transition temperature T_c as a function of hole doping from half filling (d^9) for the 438 compounds. The red squares give the estimate based on boson condensation temperature. The blue circles represent the estimate based on weak-coupling BCS theory. For a detailed account of the methods used to obtain the two estimates please consult Ref. [31]. (b) Closeup view of (a). Note that the narrow underdoped region is due to the relatively large intralayer NN hopping as compared to the intralayer exchange $J_\parallel$. A similar plot is obtained for electron doping.

hole- versus electron doping can be traced to the p-h anisotropy of the bands shown in Fig. 2(b). Similarly, the distinction between the three Ni sectors for larger hole dopings can be attributed to the distinct fillings in two of the orbitals versus the third. These different fillings are due to the interlayer hopping and exchange coupling, together with the reflection symmetry about the middle plane. Within our approximations, small rare-earth pockets start to emerge beyond an electron doping of 0.1 relative to the CeR_3NiO_8 (d^9) configuration. As shown in Fig. 3, the dominant pairing amplitude is already suppressed in this doping regime and we do not expect any significant modifications to our results due to these small pockets. We also note that the pairing in all three Ni sectors occurs with a zero relative phase, thus preserving the point-group and time-reversal symmetries. In Fig. 3(b), the $d_{x^2-y^2}$ gap of the Ni sector is plotted for the 438's as a function of doping in comparison to that of the 112 materials. Remarkably, the pairing amplitude in the 438 systems is roughly four times larger than in the 112s.

In order to estimate the superconducting transition temperature T_c, we follow a procedure analogous to that for the $t - J$ model in the case of the cuprates [25,38]. For the underdoped regime, $\delta_\alpha \to 0$, we estimate T_c as the highest boson condensation temperature of the three Ni sectors. For the overdoped regime, T_c is estimated via the value of the highest $d_{x^2-y^2}$ gap parameter at $T = 0$ using weak-coupling Bardeen-Cooper-Schrieffer (BCS) theory [39].

In Fig. 4, we plot the estimates for the T_c versus hole doping of the Ni orbitals with respect to the half-filled system $CePr_3Ni_3O_8$. The red line is the estimate based on boson condensation, while the blue line indicates the estimate based on weak-coupling BCS theory. The slope of the boson condensation temperature can also be estimated based on the analytical results for free bosons with weak dispersion along the z axis, as in the case of the cuprates [40]. The very narrow underdoped region is due to a relatively large intralayer NN hopping as compared to the intralayer exchange coupling $J_\parallel$. For a more detailed account of these estimates please consult Ref. [31]. A similar plot is obtained for electron doping. A maximum $T_c \sim 90$ K upon hole doping (from half filling) is found in the 438 materials, much larger than the $T_c \sim 15$ K observed in Sr-doped $NdNiO_2$. These results show that the $n = 3$ (438) members of the layered nickelate family are even more promising candidates for superconductivity than the recently discovered infinite-layer superconductor (hole-doped 112). Both of them exhibit a dominant pairing instability in the $d_{x^2-y^2}$ channel but the $n = 3$ material shows a pairing amplitude four times larger than that of the 112 systems and could potentially achieve a $T_c \sim 90$ K.

Our model for the 112's overestimates T_c, particularly near the Ni half-filling [31]. This further supports our main prediction—T_c in the case of the doped 438's is likely much larger than in that of the 112's.

To summarize, we have studied the electronic structure and superconducting instabilities of trilayer (438) nickelates and compared them to the recently-discovered infinite-layer superconductor (hole-doped 112). A DFT-based analysis of the 438 compounds indicates that these materials are much more cupratelike than their 112 counterparts—they exhibit a superexchange interaction which approaches a value typical of the cuprate family (as a consequence of smaller $p-d$ charge transfer energy), and a single band of Ni-$d_{x^2-y^2}$ character is around the Fermi level (without rare-earth d bands). The solutions of the corresponding $t-J$ models at the mean-field level reveal that the dominant pairing in the $d_{x^2-y^2}$ channel is significantly stronger in the 438 versus 112 materials making these materials promising superconductors if electron doping can be achieved.

O.E. and A.S.B. acknowledge NSF-DMR-1904716. E.M.N. and J.K. acknowledge ASU for startup funds. We acknowledge the ASU Research Computing Center for HPC resources. Work at Rice was supported by the DOE BES Award No. DE-SC0018197 and the Robert A. Welch Foundation Grant No. C-1411.

[1] M. R. Norman, Rep. Prog. Phys. **79**, 074502 (2016).
[2] V. I. Anisimov, D. Bukhvalov, and T. M. Rice, Phys. Rev. B **59**, 7901 (1999).
[3] M. Crespin, P. Levitz, and L. Gatineau, J. Chem. Soc., Faraday Trans. 2 **79**, 1181 (1983).
[4] M. A. Hayward, M. A. Green, M. J. Rosseinsky, and J. Sloan, J. Am. Chem. Soc. **121**, 8843 (1999).
[5] M. Hayward and M. Rosseinsky, Solid State Sci. **5**, 839 (2003).
[6] A. Ikeda, T. Manabe, and M. Naito, Physica C: Superconductivity **495**, 134 (2013).
[7] A. Ikeda, Y. Krockenberger, H. Irie, M. Naito, and H. Yamamoto, Appl. Phys. Express **9**, 061101 (2016).
[8] D. Li, K. Lee, B. Y. Wang, M. Osada, S. Crossley, H. R. Lee, Y. Cui, Y. Hikita, and H. Y. Hwang, Nature (London) **572**, 624 (2019).
[9] K.-W. Lee and W. E. Pickett, Phys. Rev. B **70**, 165109 (2004).
[10] A. S. Botana and M. R. Norman, Phys. Rev. X **10**, 011024 (2020).
[11] Y. Nomura, M. Hirayama, T. Tadano, Y. Yoshimoto, K. Nakamura, and R. Arita, Phys. Rev. B **100**, 205138 (2019).
[12] M. Hepting, D. Li, C. J. Jia, H. Lu, E. Paris, Y. Tseng, X. Feng, M. Osada, E. Been, Y. Hikita, Y. D. Chuang, Z. Hussain, K. J. Zhou, A. Nag, M. Garcia-Fernandez, M. Rossi, H. Y. Huang, D. J. Huang, Z. X. Shen, T. Schmitt, H. Y. Hwang, B. Moritz, J. Zaanen, T. P. Devereaux, and W. S. Lee, Nat. Mater. **19**, 381 (2020).
[13] G.-M. Zhang, Y.-f. Yang, and F.-C. Zhang, Phys. Rev. B **101**, 020501(R) (2020).
[14] X. Wu, D. Di Sante, T. Schwemmer, W. Hanke, H. Y. Hwang, S. Raghu, and R. Thomale, Phys. Rev. B **101**, 060504(R) (2020).
[15] H. Zhang, L. Jin, S. Wang, B. Xi, X. Shi, F. Ye, and J.-W. Mei, Phys. Rev. Research **2**, 013214 (2020).
[16] P. Jiang, L. Si, Z. Liao, and Z. Zhong, Phys. Rev. B **100**, 201106(R) (2019).
[17] F. Lechermann, Phys. Rev. B **101**, 081110(R) (2020).
[18] M.-Y. Choi, K.-W. Lee, and W. E. Pickett, Phys. Rev. B **101**, 020503(R) (2020).
[19] H. Sakakibara, H. Usui, K. Suzuki, T. Kotani, H. Aoki, and K. Kuroki, arXiv:1909.00060.
[20] F. Bernardini and A. Cano, J. Phys. Mat. (2020).
[21] V. V. Poltavets, K. A. Lokshin, M. Croft, T. K. Mandal, T. Egami, and M. Greenblatt, Inorg. Chem. **46**, 10887 (2007).
[22] V. V. Poltavets, K. A. Lokshin, S. Dikmen, M. Croft, T. Egami, and M. Greenblatt, J. Am. Chem. Soc. **128**, 9050 (2006).
[23] J. Zhang, A. S. Botana, J. W. Freeland, D. Phelan, H. Zheng, V. Pardo, M. R. Norman, and J. F. Mitchell, Nat. Phys. **13**, 864 (2017).
[24] A. S. Botana, V. Pardo, and M. R. Norman, Phys. Rev. Materials **1**, 021801 (2017).
[25] P. A. Lee, N. Nagaosa, and X.-G. Wen, Rev. Mod. Phys. **78**, 17 (2006).
[26] T. Miyatake, S. Shibutani, K. Hamada, J. Gouchi, Y. Uwatoko, K. Wakiya, I. Umehara, and M. Uehara, in *Proceedings of the International Conference on Strongly Correlated Electron Systems (SCES 2019)*.
[27] A. Nakata, S. Yano, H. Yamamoto, S. Sakura, Y. Kimishima, and M. Uehara, Adv. Cond. Matter Phys. **2016**, 5808029 (2016).
[28] K. Kobayashi, H. Yamamoto, A. Nakata, I. Umehara, M. Uehara, H. Yamamoto, A. Nakata, I. Umehara, and M. Uehara, JJAP Conf. Proc. **6**, 011106 (2017).
[29] P. Blaha, K. Schwarz, G. K. H. Madsen, D. Kvasnicka, and J. Luitz, *WIEN2K, An Augmented Plane Wave Plus Local Orbitals Program for Calculating Crystal Properties* (Vienna University of Technology, Austria, 2001).
[30] J. P. Perdew, K. Burke, and M. Ernzerhof, Phys. Rev. Lett. **77**, 3865 (1996).
[31] See Supplemental Material at http://link.aps.org/supplemental/10.1103/PhysRevB.102.020504 for detailed accounts of the electronic structure and Wannier functions calculations, $t-J$ models and their solutions at mean-field level, and estimates of T_c [41–48].
[32] A. A. Mostofi, J. R. Yates, G. Pizzi, Y.-S. Lee, I. Souza, D. Vanderbilt, and N. Marzari, Comput. Phys. Commun. **185**, 2309 (2014).
[33] J. Kunes, R. Arita, P. Wissgott, A. Toschi, H. Ikeda, and K. Held, Comput. Phys. Commun. **181**, 1888 (2010).
[34] Y. Lan, J. Qin, and S. Feng, Physica B: Condensed Matter **403**, 1032 (2008).
[35] Y. Fu, L. Wang, H. Cheng, S. Pei, X. Zhou, J. Chen, S. Wang, R. Zhao, W. Jiang, C. Liu, M. Huang, X. Wang, Y. Zhao, D. Yu, S. Wang, and J.-W. Mei, arXiv:1911.03177.
[36] D. I. Khomskii, *Transition Metal Compounds* (Cambridge University Press, Cambridge, 2014).

[37] A. K. McMahan, R. M. Martin, and S. Satpathy, Phys. Rev. B **38**, 6650 (1988).
[38] G. Kotliar and J. Liu, Phys. Rev. B **38**, 5142 (1988).
[39] H. Won and K. Maki, Phys. Rev. B **49**, 1397 (1994).
[40] X.-G. Wen and R. Kan, Phys. Rev. B **37**, 595 (1988).
[41] L. Ioffe and A. Millis, J. Phys. Chem. Solids **63**, 2259 (2002).
[42] A. J. Millis and P. A. Lee, Phys. Rev. B **35**, 3394 (1987).
[43] P. Coleman, Phys. Rev. B **35**, 5072 (1987).
[44] R. J. Gooding, K. J. E. Vos, and P. W. Leung, Phys. Rev. B **50**, 12866 (1994).
[45] J. Brinckmann and P. A. Lee, Phys. Rev. B **65**, 014502 (2001).
[46] A. Auerbach and K. Levin, Phys. Rev. Lett. **57**, 877 (1986).
[47] P. A. Lee and X.-G. Wen, Phys. Rev. Lett. **78**, 4111 (1997).
[48] N. Marzari, A. A. Mostofi, J. R. Yates, I. Souza, and D. Vanderbilt, Rev. Mod. Phys. **84**, 1419 (2012).